Seafloor displacement at Kumano-nada caused by the 2004 off Kii Peninsula earthquakes, detected through repeated GPS/Acoustic surveys

Motoyuki Kido[1], Hiromi Fujimoto[1], Satoshi Miura[1], Yukihito Osada[1], Kentaro Tsuka[2], and Takao Tabei[2]

[1]*RCPEV, Graduate School of Science, Tohoku University, Aoba-ku, Sendai 980-8578, Japan*
[2]*Natural Env. Sci., Kochi University, Akebono-cho, Kochi 780-8520, Japan*

(Received January 24, 2006; Revised March 13, 2006; Accepted March 15, 2006; Online published July 26, 2006)

In 2004, we started monitoring crustal deformation at Kumano-nada in the Nankai trough using the GPS/Acoustic technique. We observed a large southward seafloor displacement of ∼30 cm associated with the off Kii Peninsula earthquake, which occurred in September 2004, between our two survey campaigns in August and November 2004. The observed seafloor displacement is larger than that predicted from a slip model derived solely from GPS measurements on land. This may indicate the earthquake fault is slightly shallower and extends move to the NW than previously estimated.

Key words: GPS/Acoustic measurement, seafloor displacement, Kumano-nada, 2004 off Kii Peninsula earthquake.

1. Introduction

Recent development of the GPS geodetic technique and wide spreading GPS network array, like the GEONET, have revealed semi-realtime crustal deformations throughout the Japan Island (Sagiya, 2004). These deformations are the sum of episodic component due to earthquakes and long-term secular component due to the surrounding plate motions. To understand subduction processes and induced earthquake mechanisms, it is crucial to monitor the accumulation of stresses within the crust. Large inter-plate earthquakes, which periodically cause disaster to human activities, occur mostly along trenches deep under oceans. In situ monitoring of crustal deformation at the seafloor near the trenches is potentially more sensitive to possible signs of such earthquakes than data acquired on land.

The GPS/Acoustic technique for measuring seafloor displacement was first developed by a group at SIO (Scripps Institution of Oceanography), combining acoustic ranging between a transducer at the sea-surface and PXP(s) (precision transponder) on the seafloor. The position of the fluctuating surface transducer is determined by kinematic GPS analysis relative to reference station(s) on land (Spiess, 1985; Spiess *et al.*, 1998). In Japan, a several research groups have applied this technique to the subduction zones along the Japan trench and the Nankai trough, where complex distribution of asperities is expected. Along the Japan trench, repeated surveys through several years have detected inter-seismic deformation, which is consistent with that expected from the subduction rate (9.2 cm/yr) of the Pacific plate (*e.g.*, Fujita *et al.*, 2006; Funakoshi *et al.*, 2005).

Along the Nankai trough, three research groups, JHOD (Hydrographic and Oceanographic Department, Japan Coast Guard) & IIS (Institute Industrial Science, Univ. Tokyo), Nagoya Univ., and Tohoku Univ. independently have their own seafloor stations at Kumano-nada region (*e.g.*, Asada and Yubuki, 2001). Unlike at the Japan trench, no inter-seismic deformation has been observed yet mainly due to the smaller convergence rate of ∼4 cm/yr (Seno *et al.*, 1993). However, a large earthquake (M_w=7.5) occurred on September 5, 2004 in Kumano-nada. The earthquake ruptured along shallow fault that extends close (<10 km) to our seafloor station (Fig. 1) and likely resulted in a large coseismic displacement at the station. The above groups have observed the displacement and reported their initial results at recent meetings (Tadokoro *et al.*, 2005; Kido *et al.*, 2005). Fortunately, the stations are located close to the expected fault with well distributed positions relative to the fault, that should provide good constraint on inferring the fault model.

In this paper, we report results from our two surveys, one before and one after the earthquake. We use these data to constrain the extent of the fault rupture.

2. GPS/Acoustic surveys

We adopt the SIO approach (Spiess *et al.*, 1998), which uses three or more PXPs as an array. First, individual PXP position is determined by a moving acoustic survey around each PXP. Then, exact array position relative to above determined array is estimated by a fixed-point survey near the array center, which simultaneously makes acoustic measurements to all the PXPs under the assumption that the pre-determined array geometry is unchanged. A significant advantage of this method is that apparent *horizontal* position of the array is mostly free from time variation of sound velocity in seawater to the degree that sound speed structure is laterally stratified (Spiess, 1985). In addition, the relative array position between survey campaigns is not affected by

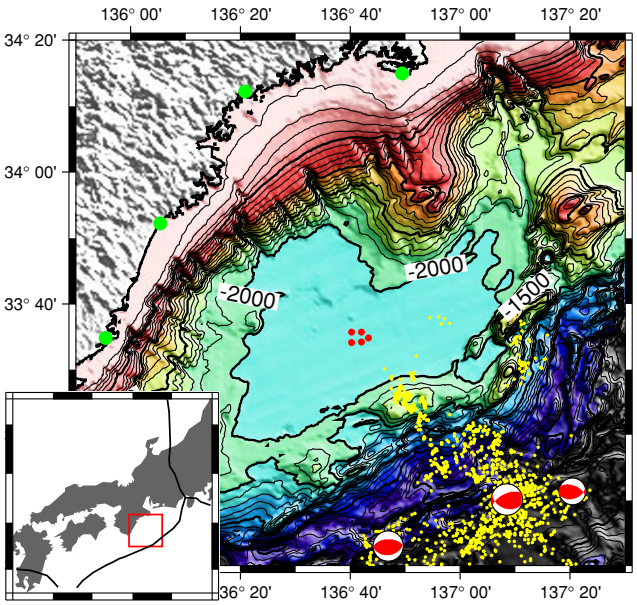

Fig. 1. Survey area. Red points are five PXPs, green points four GPS reference stations, and yellow points the aftershock activity from September 14 to October 12, 2004 (Sakai *et al.*, 2005). Focal mechanisms of the foreshock, main shock, and largest aftershock (aligned from the west) are also indicated.

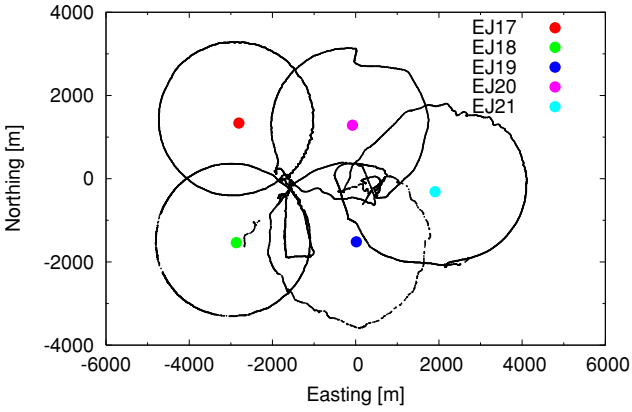

Fig. 2. Track of the buoy during the moving survey around the five PXPs from August 2004.

uncertainty of the pre-determined position and geometry of the array. Our survey method differs slightly from the SIO approach. We mount the transducer on a buoy towed from a ship while SIO mounts the transducer at the bottom of their research vessel.

The two surveys in 2004 were conducted from August 3 to 14 (labeled as AUG) and from November 2 to 12 (NOV), using a tugboat named *Choyo-maru* (Dokai Marine Systems Ltd., 268 ton; 36 m long), which could tow the buoy within a circle of 50 m radius in sea condition of a complex current. In AUG, we first determined the individual PXP positions by circling each PXP to define array geometries. We then conducted the fixed-point surveys at the two PXP array centers to measure exact array positions relative to the pre-determined positions. In NOV, only the fixed-point surveys were repeated.

2.1 Survey area

The target area of this research is Kumano-nada, which is a flat basin that developed land-ward of the Nankai trough (Fig. 1). Here the Philippine Sea plate subducts beneath the west part of the Japanese Islands with a convergence rate of 4 cm/yr (Seno *et al.*, 1993). The Nankai trough is one of the most active regions of inter-plate earthquakes, which repeatedly devastate the area (*e.g.*, Ando, 1975). Extending the monitoring of crustal deformation from land to the seafloor close to the trench is important to understand subduction in this region.

2.2 Kinematic GPS

Precise position of the transducer mounted beneath the buoy is estimated through kinematic GPS analysis of four GPS antennas on the buoy. We employed the GIPSY OASIS II software (Stephen *et al.*, 1996) to simultaneously solve 1 Hz positions of the four antennas on the buoy relative to four reference GPS stations on land (indicated by green points in Fig. 1), whose positions are calculated independently using PPP (Precise Point Positioning; Zumberge *et al.*, 1997) analysis. The 1 Hz data of the reference stations were provided from the GSI (Geographical Survey Institute). We confirmed that our PPP analyses for the reference stations coincide with GSI's official results within a few mms.

Positions of the transducer at times of each acoustic transmission and reception are interpolated from the 1 Hz positions. Considering typical frequency (∼0.5 Hz) and amplitude (∼1 m) of buoy motion, errors in the interpolation amount to 10–20 cm. However, this large error behaves randomly and effect on the final estimate of the array position is reduced with a long time span of data.

2.3 Individual PXP positioning

We installed five PXPs (EJ17–21) on the seafloor to form two arrays; a square at the west and a triangle at the east (Fig. 2). During the moving survey, we towed the buoy in a rough circle around each PXP to obtain well-distributed data. This ensures that position estimate of each PXP is not biased by differences in survey tracks. For the stability of the buoy, towing speed was kept to less than 2 knot against the water. Depending on current conditions, it took up to several hours to complete each circle track.

The transducer emits an acoustic signal every 10 s, which amounted to 11012 pings during the moving survey. All PXPs respond to the interrogation signal from the buoy. Because of the proximity of the PXPs, this meant PXPs would routinely reply while the circle was being driven around a different PXP. This resulted in 5000–6000 traveltime data for each PXP. With an assumption that sound velocity structure is laterally stratified, we can solve simultaneously for the positions of all PXPs and the time variation of the sound velocity by minimizing the misfit between observed and synthetic traveltimes.

Precision of the calculated positions of PXPs is difficult to evaluate. However, RMS misfit of traveltimes reduces from 1 ms to 0.2 ms (∼10 cm in slant range) by including the estimation of the common sound velocity variation. Furthermore, the difference between array positions estimated from the moving and from the fixed-point surveys

Table 1. Observed displacement of the two PXP arrays from August to November 2004. Locations are the center of each array.

Array	Lon	Lat	Easting	Northing
Square	136°41.063′	33°34.922′	0.7±6.4 cm	−25.4±6.4 cm
Triangle	136°42.285′	33°34.948′	8.6±3.8 cm	−33.3±4.4 cm
Average	136°41.674′	33°34.935′	4.7 cm	−29.4 cm

within the same campaign, which directly indicates the mispositioning of the PXPs, is 5–6 cm as shown in Fig. 3(c) in the next section. Therefore, precision of the individual PXP positioning can be considered as on order of ∼10 cm. It should be noted that error in the individual PXP position is nearly insensitive to shift in the apparent array position between two survey campaigns because the error always results in the same effect on array positionings for any campaigns.

2.4 Positioning of the PXP arrays

We conducted fixed-point surveys at the centers of the square and triangle arrays both in the AUG and NOV campaigns. Two days of survey time was assigned to each array in each campaign.

A single ping transmitted from the transducer reaches all the PXPs within the array, and reply signals from the PXPs are observed at slightly different time relative to each other depending on the buoy's location within the array. When traveltimes of two PXPs are too close, one can transmit an acoustic command of hardware delay to one of the PXPs in order to avoid return signals overlapping.

Array position is estimated for each single ping as a time series. Under the condition that the PXP array geometry and its depth, pre-determined by the moving survey, are fixed, one can calculate apparent *horizontal* array position for each ping as a deviation from the pre-determined position by minimizing differences of normalized traveltime residuals of three or more PXPs as

$$\sum_{k=1}^{K}\left(dT_k\cos\xi_k - dT_{k+1}\cos\xi_{k+1}\right)^2 \longrightarrow \text{minimize}, \quad (1)$$

rather than minimizing traveltime residuals themselves. In the equation, dT_k is a traveltime residual between observation and synthetic for the kth PXP. When $k = K$, the number of PXPs consisting the array, k+1 is interpreted as 1 so that PXP ID to be cyclic. The $\cos\xi_k$ is a normalizing factor to be a vertical component, where ξ_k is an emission angle of ray path measured from the vertical to kth PXP. Quantity of Eq. (1) will be zero for a case of three PXPs and will have a finite value for four or more PXPs, *i.e.* overdetermined least squares problem. Taking the strategy of Eq. (1), uncertainty of sound velocity does not affect the apparent horizontal position, and can be estimated instead.

Although more than 10000 pings were made for each fixed-point surveys of 2 days period, only 1000–2000 pings were employed, which satisfied a condition that all of PXPs of the array responded with a peak amplitude of correlogram with transmitted signal to be high enough. This low survival rate was caused by a broken sound hood attached to the transducer (the problem has been corrected). The estimated array positions relative to the pre-determined position are plotted in easting and northing components as time series in Fig. 3(a). For comparison of changes in the array position between the two campaigns, AUG and NOV, the time series data are projected on the easting/northing map for each array (Fig. 3(b)). It is clear that a large south-ward displacement of approximately 30 cm is detected in both the arrays. Upon examining the time series data, the apparent array positions show random scatter with short period and fluctuation with 15–30 min. timescales. The former scatter is mostly due to the interpolation of the transducer position from the 1 Hz data, and partly due to KGPS scattering and acoustic ranging errors. The latter fluctuation is likely due to disruption of the stratification of sound velocity structure associated with internal waves in seawater passing through the survey site. These scatter and fluctuation behave as nearly random noise for time span much longer than their typical time periods. Therefore we averaged the array position every 2 hours giving 24 2-hours estimates for each array as shown by black triangles in Fig. 3. We then average the 2-hours averages and calculate the RMS deviations which are used as error-bars in Fig. 3(c). Since the square and triangle arrays are adjacent to each other, we employed the averaged value of the two vectors as a representative observed displacement at this site. The results are summarized in Table 1.

3. The off Kii Peninsula earthquake

The off Kii Peninsula earthquake is composed of multiple ruptures within the subducting plate, and its mechanisms are quite different from typical inter-plate earthquakes (*e.g.,* Ito *et al.*, 2005; Hara, 2005). Most crustal displacements observed by land-based GPS network can be explained by two major faults; one is along the trench (referred to as Fault A) and the other along the NW extending after-shock swarm (Fault B) (GSI, 2004; Hashimoto *et al.*, 2005).

GSI (2004) reported a set of fault models $A\&B_G$ derived from their GPS analysis shown in Table 2. With this GSI model, crustal displacement at our survey site calculated using Okada's (1992) formula is 10 cm southward (Fig. 4(a)), which is significantly less than our observed displacement. However, displacement on land more than 100 km away from the faults is rather insensitive to the detailed location of the faults. On the contrary, our survey site is within a few kms of the north end of the fault B, where the displacement vector strongly depends on the position of the fault. In Fig. 4(b), we present a possible example of a modified fault model, $A\&B_M$, defined in Table 2, which roughly satisfies our observation while displacements on land are almost unchanged. This also matches observed results of Nagoya Univ. (∼21 cm SSE: Tadokoro *et al.*, 2005) and JHOD (∼6.5 cm WSW in preliminary: Fujita, personal co-

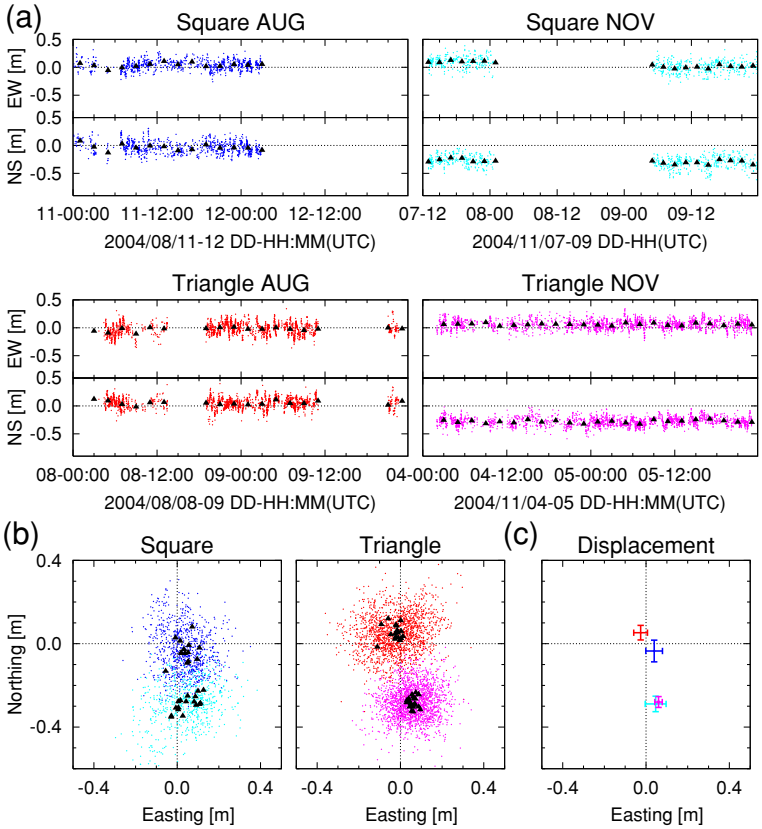

Fig. 3. (a) Time series of the estimated array positions of each ping relative to the pre-determined position for the two arrays and the two campaign periods. Easting and northing components are plotted separately. 2-hours averages of the array positions are also indicated by black triangles. (b) Projection of (a) into a map view. Results of the two campaigns are plotted in the same map to clarify the displacement. (c) Average of the 2-hours averages of (b) with its standard deviations as error bars. Symbols are plotted with identical colors among panels.

Table 2. Parameters for rectangular faults with uniform slip employed in this study. Fault B_M is modified to extend to the NW with a narrower fault width than B_G so that the total moment is preserved.

Fault	Lon [deg]	Lat [deg]	Depth [km]	Length [km]	Width [km]	Strike [deg]	Dip [deg]	Rake [deg]	Slip [m]
A	137.20	33.22	32.0	66.5	23.5	244	56	67	3.26
B_G	137.24	33.14	29.4	54.7	21.4	321	82	143	1.25
B_M	137.24	33.14	16.5	70.0	16.7	308	82	143	1.25

munication). Fault B_M extends to the NW close to our survey site and shifts shallower closer to the seafloor compared to fault B_G.

4. Discussions

The observed displacements of the square and triangle arrays shown in Table 1 differ by approximately 8 cm in the east and 8 cm in the west components. Considering the error bars range from 4 to 6 cm (Fig. 3(c)), the difference between the two arrays may not be significant. Strong horizontal gradient in displacement vector field or local seafloor deformation is required to account for the difference between the two adjacent arrays. Shallow fault activities near the survey site, like the fault B_M, may have a potential to produce the needed surface deformations. Actually, existance of mud volcanoes in this region (Nakamura *et al.*, 2005) indicates such avtivity at least in geo-

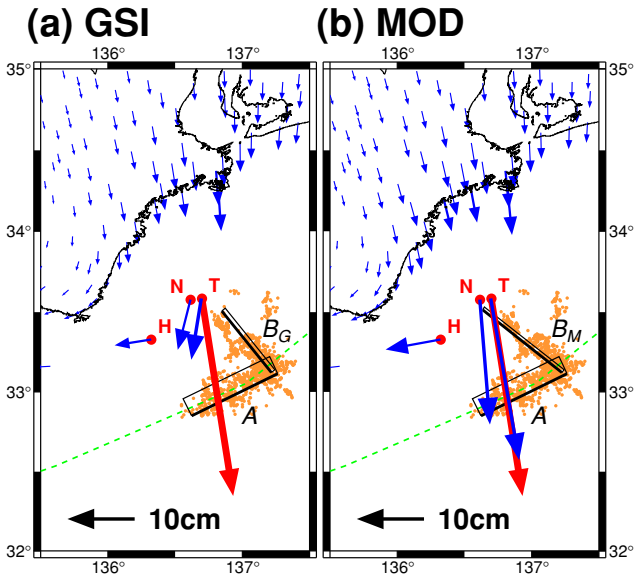

Fig. 4. Calculated displacement vectors (blue arrows) for fault models (a) $A\&B_G$ (GSI, 2004) and (b) $A\&B_M$ (this study), listed in Table 2, using the computation algorithm provided by Feigl and Dupre (1999). T, N, H indicate seafloor stations of Tohoku Univ., Nagoya Univ., and JHOD, respectively. The red arrow is the average of the observed displacements for the square and triangle arrays. Aftershock activities (orange circles) are identical those in Fig. 1. Green dashed line is the trench axis.

logical timescale. We are planning a submersible survey to find any evidence of such defomation as well as to verify the stability of mounting condition of PXPs.

Our reported uncertainties are derived from campaigns lasting 2 days and may not contain errors due to longer time-scale effects. Gagnon *et al.* (2005) reported that after several days of data collection, the precision reaches 1 cm in their application survey at the Peru-Chile trench. However, Kumano-nada region is known as a corridor of the *Kuroshio*, a strong ocean current, which has a possibility to disturb the laterally stratified sound velocity structure with a very long timescale. In addition, long base-line kinematic GPS analysis sometimes fails in centimeter-level precision. For these reasons, we consider that the difference in the displacements for the square and triangle arrays is not significant and instead we average the values of the square and triangle array for use for the red arrow in Fig. 4.

The fault model $A\&B_M$ is not optimum to satisfy the observed displacement vectors, since we derived it using forward estimation. However, the misfit to the observed displacements on seafloor is reduced significantly compared to that with $A\&B_G$. This indicates that incorporation of displacement observations at seafloor plays the important role to the fault model constraint. Therefore we consider $A\&B_M$ is a better candidate of the fault model. Introducing an inversion technique may reduce the data misfit. However, considering the limit of the data precision and oversimplification of the fault, it is questionable whether further optimization only to the displacement data gives a realistic fault model. It should be more productive to conduct a joint inversion with other observables (*e.g.*, Kusunose *et al.*, 2005) from analytic side, and to improve the precision of the GPS/Acoustic technique or construct more seafloor stations from observation side.

Acknowledgments. The authors thank to crew members on the Choyo-maru of Dokai Marine Systems Ltd. and Kaiyo-denshi Co. Ltd. for their committed assistance for the survey cruises. Suggestions by reviewers, Dr. C. David Chadwell and Dr. Masayuki Fujita, greatly improved this manuscript. The 1 Hz sampling GPS data at the reference stations on land are provided by GSI through the contract collaboration between GSI and RCPEV, Tohoku Univ. Hypocentral distribution data for the aftershocks are provided by Dr. Shin'ichi Sakai. This research is supported by *Research Revolution 2002* program, MEXT, Japan.

References

Ando, M., Source mechanisms and tectonic significance of historical earthquakes along the Nankai Trough, Japan, *Tectonophys.*, **27**, 119–140, 1975.

Asada, A. and T. Yabuki, Centimeter-level positioning on the seafloor, *Proc. Japan Acad.*, **77(B)**, 7–12, 2001.

Feigl, K. L. and E. Dupre, RNGCHN: a program to calculate displacement components from dislocations in an elastic half-space with applications for modeling geodetic measurements of crustal deformation, *Computers & Geosciences*, **25**, 695–704, 1999.

Fujita, M., T. Ishikawa, M. Mochizuki, M. Sato, S. Toyama, M. Katayama, K. Kawai, Y. Matsumoto, T. Yabuki, A. Asada, and O. L. Colombo, GPS/Acoustic seafloor geodetic observation: method of data analysis and its application, *Earth Planets Space*, **58**, 265–275, 2006.

Funakoshi, M., Y. Osada, S. Miura, M. Nishino, A. Kuwano, R. Hino, and H. Fujimoto, Initial results of GPS/Acoustic seafloor positioning using a small towed buoy off Miyagi Prefecture, northern Japan, *J. Geod. Soc. Japan*, 2005 (in Japanese) (submitted).

Gagnon, K., C. D. Chadwell, and E. Norabuena, Measuring the onset of locking in the Peru-Chile trench with GPS and acoustic measurements, *Nature*, **434**, 205–208, 2005.

Geographical Survey Institute (GSI), The earthquake SE off Kii peninsula on September 5, in the summary of the 159 meeting of the Coord. Com. Earthq. Pred., http://cais.gsi.go.jp/YOCHIREN/JIS/159/index159.html, 2004.

Hara, T., Change of the source mechanism of the main shock of the 2004 off the Kii peninsula earthquakes inferred from long period body wave data, *Earth Planets Space*, **57**, 179–183, 2005.

Hashimoto, M., K. Onoue, F. Ohya, Y. Hoso, K. Segawa, K. Sato, and Y. Fujita, Crustal deformations in Kii peninsula associated with the SE off the Kii peninsula earthquake sequence of September 5, 2004 derived from dense GPS observations, *Earth Planets Space*, **57**, 185–190, 2005.

Ito, Y., T. Matsumoto, H. Kimura, H. Matsubayashi, K. Obara, and S. Sekiguchi, Spatial distribution of centroid moment tensor solutions for the 2004 off Kii peninsula earthquakes, *Earth Planets Space*, **57**, 351–356, 2005.

Kido, M., H. Fujimoto, K. Tsuka, and T. Tabei, Earthquake-induced seafloor displacement at Kumano-nada in Nankai trough, detected by repeated GPS/Acoustic surveys, *Eos Trans. AGU*, **86(52)**, Fall Meet. Suppl., Abstract G51B-0827, 2005.

Kusunose, T., Y. Tanioka, K. Satake, T. Baba, K. Hirata, S. Iwasaki, T. Kato, S. Koshimura, Y. Hasegawa, and T. Imakiire, Slip distributions of the 2004 off Kii-peninsula earthquakes (Mw 7.3, 7.5) estimated by joint inversion using tsunami waveforms and crustal deformation data, *Eos Trans. AGU*, **86(52)**, Fall Meet. Suppl., Abstract S12A-03, 2005.

Nakamura, Y., J. Ashi, S. Morita, and K. Mochizuki, Detailed seismic image of mud volcones in Kumano basin, *Eos Trans. AGU*, **86(52)**, Fall Meet. Suppl., Abstract T13B-0457, 2005.

Okada, Y., Internal deformation due to shear and tensile faults in a half-space, *Bull. Seismol. Soc. Amer.*, **82**, 1018–1040, 1992.

Sagiya, T., A decade of GEONET: 1994–2003—The continuous GPS observation in Japan and its impact on earthquake studies, *Earth Planets Space*, **56**, xxix–xli, 2004.

Sakai, S., T. Yamada, M. Shinohara, H. Hagiwara, T. Kanazawa, K. Obana, S. Kodaira, and Y. Kaneda, Urgent aftershock observation of the 2004 off the Kii Peninsula earthquake using ocean bottom seismometers, *Earth Planets Space*, **57**, 363–368, 2005.

Seno, T., S. Stein, and A. E. Grippe, A model for the motion of the Philippine Sea plate consistent with NUVEL-1 and geological data, *J. Geophys. Res.*, **98**, 17941–17948, 1993.

Spiess, F. N., Analysis of a possible seafloor strain measurement system, *Marine Geodesy*, **9**, 385–398, 1985.

Spiess, F. N., C. D. Chadwell, J. A. Hildebrand, L. E. Young, G. H. Purcell, Jr., and H. Dragert, Precise GPS/Acoustic positioning of seafloor reference points for tectonic studies, *Phys. Earth Planet. Inter.*, **108**, 101–112, 1998.

Stephen, M. L., Y. Sever, W. L. Bertiger, M. Heflin, K. Hurst, R. J. Muellerschoen, S. C. Wu, T. Yunk, and J. Zumberge, GIPSY-OASIS II: A High Precision GPS Data Processing System and General Satellite Orbit Analysis Tool, Jet Propulsion Laboratory, California Institute of Technology, Pasadena, CA, 1996.

Tadokoro, K., R. Ikuta, M. Ando, T. Okuda, S. Sugimoto, G. M. Besana, and M. Kuno, First observation of coseismic seafloor crustal deformation due to M7 class earthquakes in the Philippine Sea plate, *Eos Trans. AGU*, **86(52)**, Fall Meet. Suppl., Abstract G41A-0348, 2005.

Zumberge, J. F., M. B. Heflin, D. C. Jefferson, M. M. Watkins, and F. H. Webb, Precise point positioning for the efficient and robust analysis of GPS data from large networks, *J. Geophys. Res.*, **102**, 5005–5017, 1997.

M. Kido (e-mail: kido@aob.geophys.tohoku.ac.jp), H. Fujimoto, S. Miura, Y. Osada, K. Tsuka, and T. Tabei